Tails in Biomimetic Design: Analysis, Simulation, and Experiment

Randall Briggs, Jongwoo Lee, Matt Haberland, and Sangbae Kim

Abstract— **Animals use tails to improve locomotion performance; here we assess how the biomimetic MIT Cheetah robot can do the same. Analysis proves that for a given power and weight, tails can provide greater average torque than reaction wheels for the short times of interest in high speed running. A simple tail controller enables the cheetah to perform aerial orientation maneuvers in simulation. The MIT Cheetah robot's tail rejects an impulsive disturbance from a 'wrecking ball' in experiments. This study demonstrates that a tail will help the MIT Cheetah achieve its goal of 30mph locomotion by 2014.**

I. Introduction

The field of bio-inspired robotics continually mines nature's abundant store of solutions to engineering challenges. However, one aspect of animal motion that has not been thoroughly explored is the incredible variety of ways the tail is used in nature, including balance, swimming, flight control, running, hopping, climbing, defense, warning, courtship, and thermoregulation. Many of these examples could provide engineers with solutions to difficult unsolved problems in robot design.

Only a few robots have incorporated tails for more than aesthetic purposes or as simple fixed inertia. One of the first robots to use an active tail was the Uniroo developed at the Leg Lab [1]. This robot emulated the motion of a hopping kangaroo and actuated the tail to cancel the motion of the leg in order to maintain constant body pitch. Simple robots with tails have been used to reproduce and better understand tail motion in geckos and other lizards [2][3]. These robots demonstrated how tails could be used for orientation control during leaping and falling when no ground reaction is available. Other robots have used swinging appendages to climb stairs [4] and hop [5].

This paper's goal is to contribute to the discussion regarding which tail uses found in nature might provide solutions for various problems in robotics and how they might be implemented practically. We will begin in Section II with a brief overview of some of the notable tail uses found in nature and specifically focus on the cheetah's use of its tail during high speed running. We then turn our focus to the MIT Cheetah and present the reader with three tail use studies. In Section III, we analytically compare a tail with existing engineering solutions for applying forces and moments to a body. In Section IV, we present simulations of a controller that is able to reorient a model of the cheetah in flight to a desired landing configuration. In Section V, we present an experiment to demonstrate the utility of the tail in rejection of an impulsive disturbance, and we conclude in Section VI.

The authors are funded by the Defense Advanced Research Project Agency and are with the Biomimetic Robotics Laboratory, Department of Mechanical Engineering, Massachusetts Institute of Technology, 77 Massachusetts Avenue, Cambridge, Massachusetts, USA. Corresponding Author: Randall Briggs, sandals@mit.edu.

II. Bio-Inspiration

Biologists have for many years recorded observations of animal tail use. Graham Hickman provided a review of these uses in mammals [6]. Kangaroos are known to use their tails both as a counter-balance as they support their weight on two legs and for energy storage during hopping [7]. Dinosaurs are also believed to have used their tails for balance in standing as a gravitational moment. During walking, the tail was believed to swing laterally to maintain the yaw of the body [8]. Long prehensile tails in many species of monkeys are used for balance in climbing and navigating narrow tree branches. These tails are also capable of grabbing onto branches and can allow the monkey to swing with their weight supported [6]. The scaled giant pangolin is capable of rolling into a tight ball while using its large tail as a shield over its body. Many lizard species as well as rodents are capable of intentionally disconnecting their tails in distress to distract potential predators. Pocket gophers are believed to use their bare tails for thermoregulation to help cool their bodies [9]. Lizards have been observed using their tails in aerial maneuvers to adjust body orientation [2][3]. Kangaroo rats have been observed swinging their tail in midair to completely turn their body and begin hopping in the opposite direction. Beavers, macropods, pangolins, spider-monkeys, and giant anteaters use their tails as a third leg of a tripod when balancing on their rear legs in order to free their forelimbs for another task such as carrying objects [6].

Our inspiration to begin this investigation came largely from a video produced by the BBC showing a cheetah during a chase [10]. In this chase, the tail can be seen quickly swinging from side to the other during rapid turns. Figure 1 shows two snapshots from this footage which capture the initial and final position of the tail in one swing. We hypothesized that the tail was providing a reaction moment to help roll the body of the cheetah in midair and initiate the turn. The tail can be seen whipping over the cheetah each time a rapid turn is made in this film sequence. We wanted to explore how this might be of use in our cheetah robot and to investigate what other uses the tail might provide for roboticists. However, conventional technologies may also be suitable for providing reaction forces and torques, so first we benchmarked tails against these other technologies.

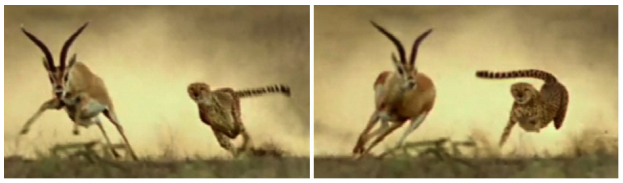

Fig. 1. Two snapshots taken from the BBC's "Life of Mammals" [10] showing the cheetah tail whip from one side to the other during a rapid turn. It is hypothesized that the tail provides a reaction moment to help roll the body of the cheetah in midair and thus assist the turn.

III. Analysis: Comparison of Biological and Artificial Force/Moment Technologies

We are interested in tails from the perspective of bio-inspired robot design. A fundamental tenant of our design philosophy is that we must not simply copy nature; rather, we seek to extract principles from biological examples for application to original designs. In this paper, we study the principle that an appendage for applying forces/moments without requiring ground contact is useful for legged locomotion. Animals use a tail for this purpose, but in engineering we should not neglect alternative mechanisms on the sole basis that they are not found in nature.

Indeed, several artificial mechanisms are used to apply forces/moments without reacting those forces against fixed solids: turbojets propel planes through the air, reaction masses stabilize skyscrapers, and gyroscopes reorient spacecraft in orbit. Table I summarizes some of these mechanisms and key properties of each.

TABLE I

Properties of force/moment application technologies:

Technology	Force	Torque	Δ CoM
Tail	Yes	Yes	Yes
Reaction Wheel [11]	No	Yes	No
Control Moment Gyroscope [11]	No	Yes	No
Reaction Mass	Yes	No	Yes
Thruster / Gas Jet [11]	Yes	No	No
Propeller [12]/ Rotor	Yes	Yes	No
Turbojet [12]/ Turbofan [12]	Yes	No	No

Capabilities of technologies to apply controlled forces and moments at their attachment point and adjust system center of mass.

Several of them are dismissed as candidates for use on the MIT Cheetah on qualitative grounds. Thrusters, turbofans, turbojets, and propellers are all very capable, but have relatively high minimum complexity for practical implementation. Gas jets are simpler, but less powerful for a given mass, and require a source of compressed gas not otherwise needed by the robot. The effectiveness of a translating reaction mass would be limited by the stroke of its linear guide, and a long linear guide is an undesirable use of space. The analysis of control moment gyroscopes is more complicated than other technologies; they deserve further study, but they are beyond the scope of this paper.

We consider in greater detail the relative advantages of a reaction wheel. As noted in [13], the principal difference between a tail and a reaction wheel is that a reaction wheel is designed to fit entirely within a volume such that it can rotate continuously, whereas a tail is allowed to have greater maximum dimensions, and thus considerably greater moment of inertia, but it cannot rotate continuously without colliding with other parts of the body or the ground.

Consider the goal of reorienting the roll angle of a cheetah's posterior to change running direction while in pursuit of evasive prey. It is hypothesized that cheetahs rapidly swing their tails to provide the moment needed to rotate their posterior, especially when the rear legs are not in contact with the ground. On the MIT Cheetah robot, either a tail or a reaction wheel could react such a moment, but we wish to quantify which is capable of applying a greater average moment over a given amount of time. It is assumed that at the end of this time, the legs will be in contact with the ground, and any angular momentum accumulated by the reaction wheel or tail can be 'dumped' to the ground through the legs.

We begin our analysis by deriving the equations of motion of the system. After finding the differential equation describing the relative rotation of the reaction wheel or tail and the robot's posterior, we will consider the torque limitation imposed by an electric actuator with a given speed/torque relationship. We will then study how the optimal design of the actuator's transmission depends on parameters such as the motor's peak power P^*, the reaction wheel or tail's effective inertia I_E, and the time of interest t_f. The result allows us to compare whether a reaction wheel or tail is more appropriate for rolling the cheetah posterior under the given constraints.

A. Equations of Motion

A tail or reaction wheel, hereafter referred to as body B, is joined to the posterior of the cheetah, body A, which is assumed to be decoupled from the rest of the cheetah by the flexibility of the spine. A rotational actuator produces torque $\mathbf{T}$ between between body A and body B. The system is split at the joint between the two bodies, and the resulting free body diagrams are shown in Figure 2.

Applying Newton's second law to body A yields

$$\sum_A \mathbf{F}_i = -m_A g\hat{\mathbf{j}} - \mathbf{R} = m_A \ddot{\mathbf{r}}_A. \tag{1}$$

Euler's second law for body A is

$$\sum_A \mathbf{T}_i = -\mathbf{T} + \mathbf{r}_{C/A} \times -\mathbf{R} = \frac{d}{dt}\left(\mathbf{I}_A \cdot \boldsymbol{\omega}_A\right). \tag{2}$$

Likewise, for body B,

$$\sum_B \mathbf{F}_i = -m_B g\hat{\mathbf{j}} + \mathbf{R} = m_B \ddot{\mathbf{r}}_B, \tag{3}$$

$$\sum_B \mathbf{T}_i = \mathbf{T} + \mathbf{r}_{C/B} \times \mathbf{R} = \frac{d}{dt}\left(\mathbf{I}_B \cdot \boldsymbol{\omega}_B\right). \tag{4}$$

Expressing $\ddot{\mathbf{r}}_B = \ddot{\mathbf{r}}_A + \ddot{\mathbf{r}}_{B/A}$, Equation 1 and Equation 3 sum and rearrange to give

$$\ddot{\mathbf{r}}_A = -g\hat{\mathbf{j}} - \frac{m_B}{m_A + m_B}\ddot{\mathbf{r}}_{B/A}. \tag{5}$$

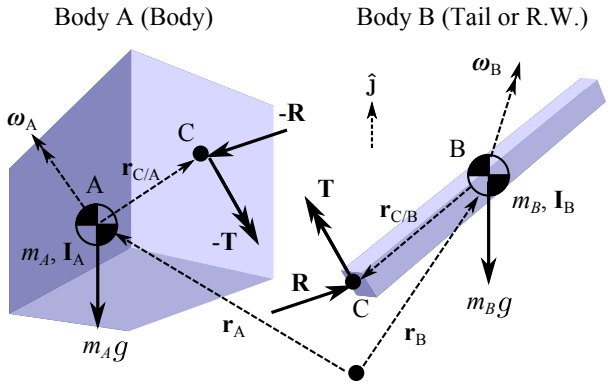

Fig. 2. Free body diagram of the posterior (body A) and tail/reaction wheel (body B). Torque $\mathbf{T}$ and force $\mathbf{R}$ act at the joint between the bodies. Center of mass points A and B are at positions $\mathbf{r}_A$ and $\mathbf{r}_B$ relative to an inertial reference; point C is at relative position $\mathbf{r}_{C/A}$ with respect to point A and $\mathbf{r}_{C/B}$ with respect to point B. Vector $\mathbf{r}_{B/A}$ (not illustrated) extends from point A to point B. Bodies A and B have masses m_A and m_B, moments of inertia relative to their respective center of masses $\mathbf{I}_A$ and $\mathbf{I}_B$, and angular velocities $\boldsymbol{\omega}_A$ and $\boldsymbol{\omega}_B$. Gravitational acceleration g acts along $-\hat{\mathbf{j}}$.

Substituting Equation 5 back into Equation 1 yields an expression for the reaction force

$$\mathbf{R} = m_E \ddot{\mathbf{r}}_{B/A}, \tag{6}$$

where $m_E = \frac{m_A m_B}{m_A + m_B}$ is the 'effective mass' of the bodies. Surely the dynamics can be derived without this constraint reaction force entering the equations explicitly, but it is instructive to see that the reaction force acting on body A is linearly proportional to the relative acceleration of B with respect to A. In the general case, this potentially complicated $\mathbf{R}$ acts at a distance from the center of mass of body A, creating a moment about the center of mass. This presents an essential difference between a reaction wheel and a tail, which is also noted in [14]. For a reaction wheel, $\ddot{\mathbf{r}}_{B/A} \equiv \mathbf{0}$, and the moment applied about body A center of mass is simply $\mathbf{T}$[1]. The motion of a tail, however, imparts a force on body A, which creates a moment about the body A center of mass. Depending on the state at each instant, this may either augment or diminish the resultant torque produced by the tail, complicating analysis considerably.

We continue by reducing our equations to the planar case and assuming that point A projects onto point C in the plane, eliminating the $\mathbf{r}_{C/A} \times -\mathbf{R}$ term of Equation 1. This simplification is justified when considering a real cheetah in the mediolateral plane M (from behind), in which the projection of the center of mass is likely to be only slightly above or below the attachment point of the tail. Also, since we are interested in biology-inspired design rather than copying biology, we are free to choose the location of the tail joint on the cheetah if we deem analytical tractability to be sufficiently important. Adding Equation 2 and Equation 4 yields

$$\mathbf{r}_{C/B} \times \mathbf{R} = I_A \dot{\omega}_A \hat{\mathbf{k}} + I_B \dot{\omega}_B \hat{\mathbf{k}}, \tag{7}$$

[1]However, $\mathbf{T}$ itself can be complicated in three dimensions, when the accumulated angular momentum of body B begets gyroscopic torques.

where some vector and tensor quantities have been replaced by their corresponding vector and scalar quantities in the plane, and $\hat{\mathbf{k}}$ is the unit vector normal to the plane M. Defining $b = \text{proj}_M\left(\mathbf{r}_{C/B}\right)$ and using Equation 6, the term $\mathbf{r}_{C/B} \times \mathbf{R}$ evaluates to $-m_E b^2 \dot{\omega}_B \hat{\mathbf{k}}$, and thus

$$I_A \dot{\omega}_A = -\left(I_B + m_e b^2\right) \dot{\omega}_B. \tag{8}$$

Note that this can be integrated, yielding a statement of angular momentum conservation,

$$I_A \omega_A + \left(I_B + m_e b^2\right) \omega_B = H, \tag{9}$$

where H is the constant of integration. If the initial angular velocities are zero, then integrating once more yields

$$\Delta\theta_A = -\frac{I_B + m_e b^2}{I_A} \Delta\theta_B, \tag{10}$$

which reveals that the change in the absolute angle of body A $\Delta\theta_A$ is linearly related to the change in angle of body B $\Delta\theta_B$ and opposite in direction.

Solving Equation 2 and Equation 4 for $\dot{\omega}_A$ and $\dot{\omega}_B$, respectively, and taking the difference, we get an equation for the relative angular acceleration

$$\dot{\omega}_B - \dot{\omega}_A = \dot{\omega} = \frac{T}{I_E}, \tag{11}$$

where $I_E = \left[\frac{I_A\left(I_B + m_E b^2\right)}{I_A + I_B + m_E b^2}\right]$ is the effective inertia of bodies A and B.

B. Actuator Limitation

Assuming the actuator, including a fixed gear transmission, has a linear speed-torque curve while operating at its maximum voltage, the maximum motor power P^* is produced at half its no load speed $\frac{\omega_0}{2}$ and half its stall torque $\frac{T_0}{2}$, that is $P^* = \frac{\omega_0 T_0}{4}$. Then the torque of the motor as a function of the speed can be expressed as

$$T = T_0 \left(1 - \frac{\omega T_0}{4P^*}\right). \tag{12}$$

Substituting this relationship into Equation 11 completes the equation of motion,

$$\dot{\omega} + \frac{\omega T_0^2}{4P^* I_E} - \frac{T_0}{I_E} = 0, \tag{13}$$

the solution of which is

$$\omega(t) = \left(\omega(0) - \frac{4P^*}{T_0}\right) e^{-\frac{T_0^2}{4P^* I_E} t} + \frac{4P^*}{T_0}. \tag{14}$$

C. Angular Impulse

We wish to design our system to maximize the average torque over time of interest t_f, which is equivalent to maximizing angular impulse, the integral of the torque over the time of interest. Assuming that the initial relative angular velocity $\omega(0) = 0$, Equation 14 is substituted into Equation 12 and integrated for the total impulse

$$J = \int_0^{t_f} T dt = \frac{4P^* I_E}{T_0} \left(1 - e^{-\frac{T_0^2}{4P^* I_E} t_f}\right), \tag{15}$$

the quantity we seek to maximize.

D. Orientation Change

It is important to note that the integral of Equation 12 can also be expressed

$$J = T_0 \left(t_f - \frac{\Delta\theta T_0}{4P^*} \right), \tag{16}$$

where $\Delta\theta = \Delta\theta_B - \Delta\theta_A$ is the relative angle between the two bodies. Equation 16 can be equated to Equation 15 and rearranged to give a closed form expression for $\Delta\theta$, which, for a tail, may need to be limited to avoid a collision with the legs or the ground. Combined with Equation 10, we also have closed form time trajectories for $\Delta\theta_A$ and $\Delta\theta_B$.

E. Optimization

In order to properly compare the reaction wheel and tail, we must maximize $J(T_0)$ for each by appropriate design of the transmission, or choice of stall torque T_0. We look for a maximum $J^* = \max_{T_0} J(T_0)$ by taking the derivative

$$\frac{dJ}{dT_0} = \left(2t_f + \frac{4I_E P^*}{T_0^2} \right) e^{-\frac{T_0^2}{4I_E P^*} t_f} - \frac{4I_E P^*}{T_0^2} \tag{17}$$

and solving $\left.\frac{dJ}{dT_0}\right|_{T_0=T_0^*} = 0$ for an extreme point. The MATLAB Symbolic Toolbox [15] provides the unique positive real solution

$$T_0^* = \sqrt{-\frac{2I_E P_0}{t_f} \left(1 + 2W_{-1}\left(-\frac{1}{2\sqrt{e}} \right) \right)}, \tag{18}$$

where W is the Lambert W-function [16], which evaluates at the given argument to $W_{-1}\left(-\frac{1}{2\sqrt{e}}\right) \approx -1.7564$. This is verified to be a maximum, as

$$\left.\frac{d^2J}{dT_0^2}\right|_{T_0=T_0^*} = -2 \left(1 + \frac{1}{W_{-1}\left(-\frac{1}{2\sqrt{e}}\right)} \right) \frac{t_f}{T_0^*} < 0. \tag{19}$$

The optimal $T_0 = T_0^*$ of Equation 18 can be substituted into Equation 16, yielding an analytical expression for maximum $J = J^*$ as a function of P^*, I_E, and t_f. A plot of this function is shown in Figure 3.

F. Discussion

This analysis provides a means for assessing whether a tail or reaction wheel is more appropriate for the given task. Given a body inertia I_A, geometry and mass constraints, and maximum power P^* that determines the motor to be used, the rest of the system can be optimized roughly as follows:

- Design a reaction wheel of maximal moment of inertia (under the constraints) that is free to rotate continuously.
- Design a maximal moment of inertia tail. Determine the maximum allowable relative rotation of the tail.
- Use Equation 18 for actuator design, that is, to determine the optimal stall torques for the tail actuator and the reaction wheel actuator.
- Use Equation 15 to determine the maximum angular impulse J^* in the time of interest t_f (and within the maximum allowable $\Delta\theta$, for the tail) of each system. The system capable of a higher impulse under the constraints is likely the better option.

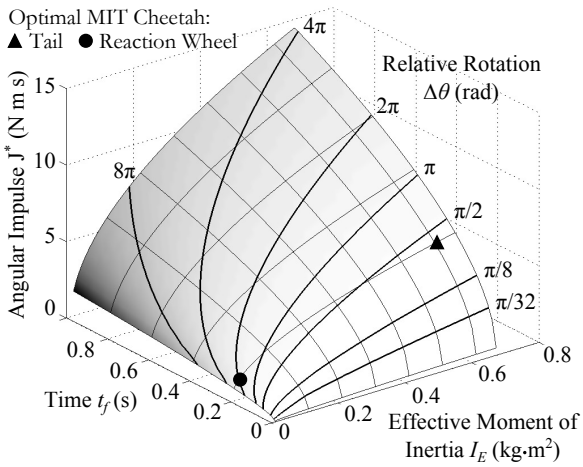

Fig. 3. Results of analysis: maximum achievable angular impulse for given maximum motor power $P^* = 200$W and body A inertia I_A = 4 kg·m^2 as a function of system effective moment of inertia I_E and time of interest t_f. Shading indicates relative angle $\Delta\theta$; lines of constant relative angle are shown. For the MIT Cheetah, the maximum mass for tail or reaction wheel is $m = 2$kg. Allowing maximum radius $r_w = 0.1$m for a reaction wheel yields $I_{E,w} \leq mr_w^2 = 0.02$kg·m^2, and allowing $r_t = 0.6$m for a tail yields $I_{E,t} \leq mr_t^2 = 0.61$kg·m^2. For the time of interest $t_f \approx 0.2$s, the optimal tail can produce a significantly higher maximum angular impulse than the reaction wheel without exceeding the maximum allowable rotation of $\Delta\theta \approx \pi/2$.

Of course, many different constraints can complicate the analysis. There is always a finite selection of motor and gearbox combinations, it is common for total system mass rather than power to drive motor selection, and adding length to a tail may simultaneously increase its moment of inertia but decrease its range of motion. Other complexities, such as a nonlinear motor speed/torque curve, and a large distance between the actuator axis and body center of mass, can preclude closed-form analysis.

Still, the preceding analysis outlines a path for numerical studies under such complications, and reveals several important trends when the assumptions made herein are nearly true.

- The maximum impulse that can be delivered over a long time period is proportional to the square root of the product of motor power, system effective moment of inertia, and time (Equations 15 and 18).
- The longer spatial dimension of a tail provides the advantage of a greater moment of inertia at the cost of a constraint on maximum allowable relative rotation.
- A reaction wheel is appropriate when there are tightly confining geometry constraints and the time of interest is very long.
- A tail is appropriate when space is available for a high moment of inertia and the time of interest is very short.

For the MIT Cheetah robot, the time of interest is very short, and there is plenty of space behind the robot for a high effective moment of inertia tail. As illustrated in Figure 3, a tail offers a considerably higher impulse in our application.

TABLE II
CHEETAH SIMULATION PARAMETERS:

Parameter	Value	Units
Body Mass	35	kg
Body CoM-Pivot	0.525	m
Body $\hat{\mathbf{x}}$ Moment	0.4	kg·m^2
Body $\hat{\mathbf{y}}$ Moment	4.0	kg·m^2
Body $\hat{\mathbf{z}}$ Moment	4.0	kg·m^2
Tail Length	0.54	m
Tail Mass	0.74	kg

Thus we move forward with our study of tails by considering how their inertial torque can be used to reorient the body during flight.

IV. SIMULATION: ATTITUDE MANEUVERS USING A TAIL

In this section, we study a controller for performing aerial orientation maneuvers in three dimensions using a tail. Attitude control using conventional engineering technologies compared in Table I is well studied for aircraft and spacecraft [17][18], and there are many studies of self-righting of animals during free fall [19][20]. There are general studies for control of two rigid bodies with three torque axes [21], and even studies of bio-inspired robots which reorient their bodies primarily about one axis [3][14] or decoupled multiple axes [2]. We present a simple feedback law for coupled pitch, roll, and yaw (three-axis) maneuvers with only two control axes.

In the context of spatial maneuvers, perhaps the most important difference between tails and conventional inertial reaction technologies is that the motion of the tail creates a reaction force per Equation 6, which adds a moment in Euler's second law for the body, Equation 2. Our approach is to neglect these reaction forces in controller design for simplicity, and test the controller's performance under the complete dynamics to determine the extent to which this simplification is justified.

A. The Plant

1) Modeling: We model the cheetah as two rigid bodies in three dimensional space as in Figure 2, but with a few notable differences. The first rigid body, representing the MIT Cheetah's body, includes the mass of all cheetah body parts other than the tail, rather than the posterior alone. The second rigid body, representing the tail, is a point mass at the end of a massless rod, which is attached to the body through a frictionless universal joint. The first axis of the universal joint is aligned with a principal axis of the body, the second axis is always perpendicular to it, and a torque actuator acts about each. Aerodynamic forces/torques are neglected due to the considerable mass of the system relative to its surface area and speed, and translational motion is not considered. Table II lists the parameters used.

2) Kinematics: XZY Euler (Cardan) angles about the body-fixed principal axes are used to describe the orientation of the body relative to the inertial frame. Since the universal joint has two degrees of freedom, two angles are used to describe the tail's orientation relative to the body. The coordinates were carefully chosen to avoid the singularities inherent to all Euler angle orientation representations.

3) Dynamics: After formulating the kinetic energy of the body in terms of the chosen angles and their time derivatives, we use Lagrange's method to derive the equations of motion using the MATLAB Symbolic Toolbox [15]. The equations are integrated using MATLAB's `ode45()` [22] function with default parameters.

B. Control

The function of the controller in this section is to use the tail to change the cheetah's body orientation while it is not in contact with the ground, such as during the aerial phase of running. Design of this controller is difficult because:

- The system is highly underactuated. We must regulate the orientation of the body in space (3 degrees of freedom) while imposing limits on the orientation of the tail (2 degrees of freedom) using only two control torques of limited magnitude.
- The three dimensional dynamics among the states are strongly coupled, highly nonlinear, and thus non-intuitive.

While our long-term goal is to develop a controller suitable for re-orienting the body in mid-air to compensate for unexpected disturbances, we simplify the problem for this initial study. The controller itself does not attempt to control the angular velocity when the desired orientation is reached, set explicit bounds on the tail orientation, or limit or actuator torques, although the latter are effectively limited by gain selection. Despite these simplification, we are still left with an underactuated system with difficult dynamics.

Without loss of generality, the desired orientation is set as where body roll, yaw and pitch are all zero. The control algorithm executed at each instant to achieve this orientation from any initial position is:

1) Find the Euler axis $\hat{\mathbf{e}}$, that is, the unique axis fixed in space about which the body could rotate to achieve the desired orientation.
2) Find the Euler axis angle θ_e, that is, the magnitude of the rotation about the Euler axis $\hat{\mathbf{e}}$ needed to achieve the desired orientation.
3) Calculate the current angular velocity $\boldsymbol{\omega}_b$ of the body and the corresponding angular momentum $\mathbf{H}_b$.
4) Define the desired angular velocity $\boldsymbol{\omega}_b^d$ to be in the direction of the Euler axis $\hat{\mathbf{e}}$ with magnitude proportional to the Euler axis angle θ_e:
$$\boldsymbol{\omega}_b^d = k_1 \theta_e \hat{\mathbf{e}}, \tag{20}$$
where k_1 is a tuned, constant gain.
5) Determine the desired angular momentum $\mathbf{H}_b^d$ to be that which corresponds with the desired angular velocity $\boldsymbol{\omega}_b^d$,
$$\mathbf{H}_b^d = \mathbf{I}_b \cdot \boldsymbol{\omega}_b^d. \tag{21}$$

6) Determine the desired change in angular momentum $\dot{\mathbf{H}}_b^d$, which is in the direction of and is proportional to the error in angular momentum. That is,

$$\dot{\mathbf{H}}_b^d = k_2 \left(\mathbf{H}_b^d - \mathbf{H}_b \right), \tag{22}$$

where k_2 is a tuned, constant gain. The desired torque $\mathbf{T}^d$ is set equal to $\dot{\mathbf{H}}_b^d$.

7) Project the desired torque onto the space of achievable torques, that is

$$\mathbf{T} = \text{proj}_S \mathbf{T}^d, \quad S = \text{span}(\mathbf{T}_1, \mathbf{T}_2), \tag{23}$$

where $\mathbf{T}_1$ and $\mathbf{T}_2$ are unit torques along the axis of the actuators.

The controller performance was improved by optimizing via single-shooting [23] the initial tail orientation and gain k_2 in Equation 22 to minimize the norm of the Euler angles of the body at the final state. This approach allowed us to specify a desired time at which the goal was to be reached, and could be extended to specify a desired final angular velocity and set limits on the final orientation of the tail. The use of onboard optimization is reasonable when compensating for known disturbances, such as slopes and uneven terrain, as the MIT Cheetah controller may plan its stride, including aerial maneuvers incorporating the tail, to compensate for these. Separating the relatively simple problem of choosing the initial orientation of the tail from the considerably more complicated problem of designing the trajectory to the goal fits well in the framework of [24] that has been studied for control of the MIT Cheetah.

C. Discussion

As shown in Figure 4, the controller fails to achieve the desired orientation when the initial tail orientation is arbitrary, but is successful when then initial tail orientation is optimized.

The simple controller has known deficiencies. As shown in Equation 6, acceleration of the tail center of mass relative to the body center of mass creates reaction forces at the joint, which in turn create moments about the body center of mass. This controller does not consider these moments when calculating the motor torque needed to adjust the body angular momentum. Using these natural dynamics will increase the input effort required from some states and decrease the required actuator torque from others. Some additional computation is required, but this may be a simple way to make the controller more effective.

Nonetheless, the experiments are enlightening. Starting from random tail orientations, the controller tends to fail by orienting the system in a 'singular equilibrium', that is, a situation in which the required torque is orthogonal to the space of achievable torques. An attempt was made to avoid this singularity by perturbing the desired angular momentum as the singularity was approached, but this was not very effective. This suggests that increasing the moment of inertia of the tail about its axis and adding a third actuator about that axis would significantly improve ease of control.

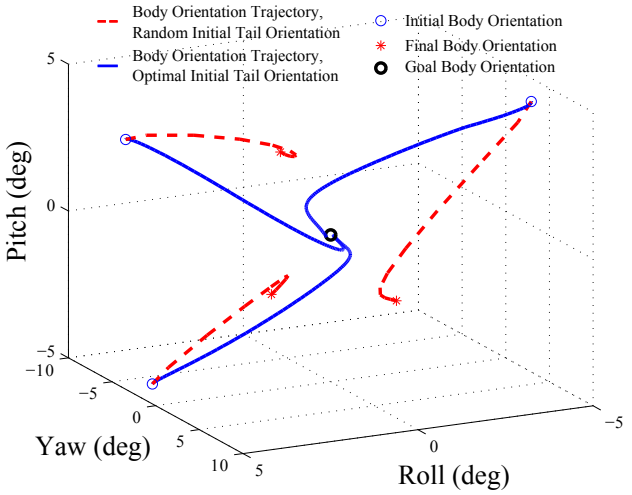

Fig. 4. Sample orientation trajectories of the controlled cheetah body from sample initial angles. Trajectories starting at random initial body and tail orientation do not reach their goal at the origin, but they do decrease the distance from the origin, that is, the norm of the Euler angles. Trajectories starting from the same body angles but with optimized initial tail angles nearly pass by the origin at a desired time. All trajectories shown are for zero angular momentum about the system center of mass; trajectories for the system with non-zero angular momentum do pass by the origin but eventually deviate.

Several items remain to be addressed before an aerial maneuver controller can be implemented on the MIT Cheetah robot. However, one tail controller has already been implemented on the MIT Cheetah robot; the simpler problem of using the tail to stabilize the robot against disturbances while feet are in contact with the ground is studied in the following section.

V. Experiment: External Disturbance Rejection using a Tail

In order to demonstrate the use of a tail for one purpose in robotics, we designed an experiment based on [25], which considers tail balance in cats. In their experiment cats were trained to walk along a narrow beam and in random cases a researcher would move the beam laterally a fixed distance while a camera observed the movement of the tail. In every case, the cat would swing the tail in the direction the beam was moved in order to maintain balance. The researchers then paralyzed the tail muscles of the cat and repeated the experiment, finding that the cats now fell from the beam far more frequently. Walker's work indicated that in situations where the legs could not be used to provide reaction forces the tail was invaluable to maintain balance.

1) Experimental Setup: In our experiment, the MIT robotic cheetah was set to stand in place while a large disturbance was introduced. Figure 5 shows an image of the experimental setup. The tail was driven by a DC motor through a 43:1 gearbox. The mass of the tail was 0.74kg and the moment of inertia about the motor rotation axis was measured to be 0.160kg m^2 based on period of oscillation.

For each trial, the feet of the cheetah were set in the same position as marked by tape on the standing platform.

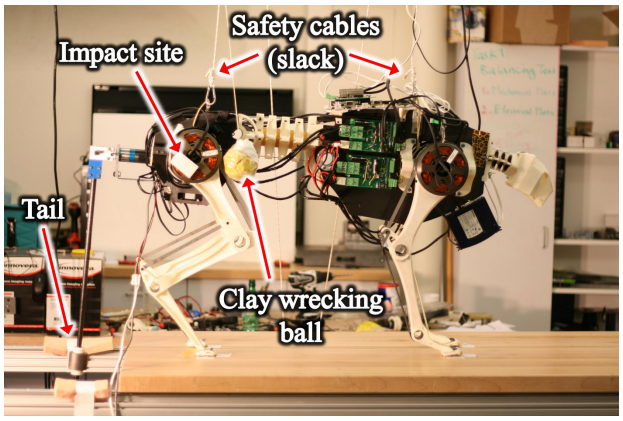

Fig. 5. Experimental setup: the robotic cheetah was set to stand while the clay wrecking ball was swung into the impact site on the rear pelvis. A foam pad was added at the impact site to soften the shock on the robot.

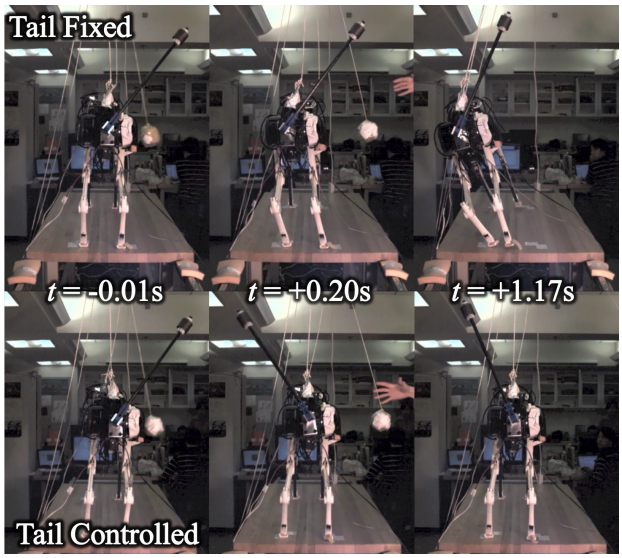

Fig. 6. Snapshots taken from two high speed videos recordings of the experiment. Tail fixed: the tail was set to hold the initial position with a stiff proportional control. Tail controlled: upon impact of the clay wrecking ball, the tail followed an open loop trajectory to stabilize the hip. A video accompanies this paper in the conference proceedings.

The body orientation was carefully adjusted to ensure the same initial conditions for each test. The servos controlling abduction of the four legs were energized and set to maintain position while the leg length and angle were mechanically locked. To apply a standard disturbance, a clay mass weighing 1.16kg was swung into the cheetah from a prescribed height in each test. Initially, the clay mass was released at different heights to find a level that would consistently knock the cheetah off balance and for all subsequent tests the same height was used. The mass hit the cheetah on the right side of the hip as shown in Figure 5 each time with a velocity of 5 ± 0.2m/s. For the swinging tail cases, the tail was initially set to a slight angle from the vertical toward the incoming clay. In cases where the tail was held fixed, the tail was set to this same angle and kept in place with a stiff proportional control. The measured acceleration caused by the impacting clay would trigger the tail to follow an open loop trajectory in order to counteract the disturbance and maintain balance of the cheetah. All tests were recorded by a high speed video camera viewing the robot from the rear. Three axes of acceleration, three axes of gyroscope output, motor current and voltage, motor position, and commanded position were all logged in each test.

2) Results and Discussion: In all but a few cases, the cheetah would lose balance when struck when the tail was inactive. Reviewing these videos showed the tail initially displaced slightly by the impact only to recover the original position soon after. The momentum of the clay was transferred to the rear hips, which swung outward over the legs until finally causing the cheetah to tip and fall into the support of the safety cables. Movement of the hips was always unidirectional in these cases. Figure 6 shows snapshots of the video taken at different times and Figure 7 shows the horizontal position of the hips as a function of time.

Figure 6 also shows snapshots of the case where the tail was swung and followed a predetermined trajectory upon impact. The trajectory was calculated to offset the momentum transfer from the clay and then was manually tuned over several trials. In Figure 7, one can see from the plot of hip displacement that the hips initially began to move with the same velocity as in the case with the passive tail. As soon as the tail began to accelerate, however, the hips quickly decelerated and moved slightly back toward the center position. After approximately 0.2s the tail reached the commanded position and began to decelerate, thus causing the hips to again accelerate outward. The cheetah did not lose balance, however, and returned to a new, shifted equilibrium stance.

Although this test was performed with the cheetah in a static stance, we believe the results to be applicable during dynamic walking and running. Mid-stride, a tail might quickly react to a disturbance or foot misplacement and keep the body stable long enough for the next foot placement can be made. The desired delay in body motion is shown in Figure 7 before the black dividing bar. This portion of the plot is almost identical among experimental trials. The plot of position difference shows a significant peak at about 0.23s where the fixed tail case has progressed about 7cm beyond the swung tail case. During running, this difference might be crucial in maintaining stability long enough for the next stride to be planned appropriately.

VI. Conclusion

In this paper we presented three focused examples investigating the use of a tail for body reorientation and disturbance rejection. We demonstrated how a tail can be more effective than a reaction wheel in reorienting the body in cases when space, power, and time are limited. We proposed a simple, state-feedback controller that was able to successfully achieve a desired landing orientation during a limited flight time in simulation. Finally, we presented the results from an

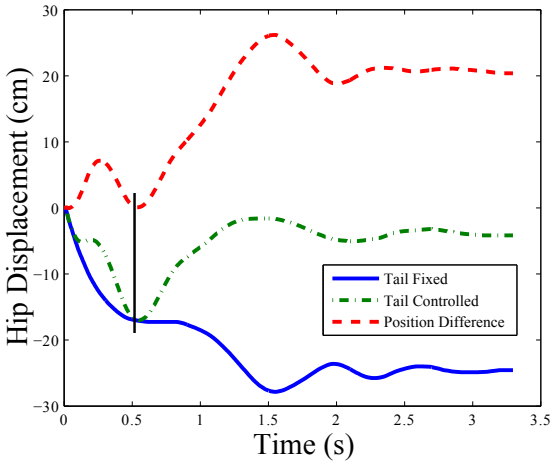

Fig. 7. Horizontal trajectory of the hip for two tests, and the difference between them. Dash-dotted line represents the horizontal position of the hips in the case with the tail actively swinging. Solid line represents the horizontal position of the hips in the case with the tail held fixed. Dashed line represents the difference in position between the two cases. Notice the peak in the difference created by the motion of the swinging tail. The swinging tail allows for more time in the stable region when a correcting foot placement can be made. The region to the left of the dividing bar is very consistent between all the experiments, whereas some variation is seen to the right.

experiment showing the effectiveness of a tail in stabilizing the body after a large disturbance is introduced. Each of these examples is the beginning of work to more completely utilize the advantages of a tail. We believe this paper has provided the reader with arguments and evidence to promote further investigation into the possibilities tails provide for improving legged robot performance.

ACKNOWLEDGEMENTS

The authors would like to thank Sang Ok Seok for support with test hardware electronics, Mojtaba Azadi for helpful discussions, and Heather Murdoch for verifying analytical calculations using *Mathematica*.

REFERENCES

[1] G. Zeglin, "Uniroo, a one legged dynamic hopping robot," B.S. thesis, Massachusetts Institute of Technology, Dept. of Mechanical Engineering, 1991.

[2] A. Jusufi, D. Kawano, T. Libby, and R. Full, "Righting and turning in mid-air using appendage inertia: reptile tails, analytical models and bio-inspired robots," *Bioinspiration & biomimetics*, vol. 5, p. 045001, 2010.

[3] T. Libby, T. Moore, E. Chang-Siu, D. Li, D. Cohen, A. Jusufi, and R. Full, "Tail-assisted pitch control in lizards, robots and dinosaurs," *Nature*, vol. 481, no. 7380, pp. 181–184, 2012.

[4] R. Hayashi and S. Tsujio, "High-performance jumping movements by pendulum-type jumping machines," in *Intelligent Robots and Systems, 2001. Proceedings. 2001 IEEE/RSJ International Conference on*, vol. 2. IEEE, 2001, pp. 722–727.

[5] F. Iida, R. Dravid, and C. Paul, "Design and control of a pendulum driven hopping robot," in *Intelligent Robots and Systems, 2002. IEEE/RSJ International Conference on*, vol. 3. IEEE, 2002, pp. 2141–2146.

[6] G. HICKMAN, "The mammalian tail: a review of functions," *Mammal Review*, vol. 9, no. 4, pp. 143–157, 1979.

[7] U. Proske, "Energy conservation by elastic storage in kangaroos," *Endeavour*, vol. 4, no. 4, pp. 148–153, 1980.

[8] A. Howell, *Speed in animals: their specialization for running and leaping*. Hafner Publishing Company New York, 1965.

[9] B. McNab, "The metabolism of fossorial rodents: a study of convergence," *Ecology*, pp. 712–733, 1966.

[10] D. Attenborough, "The life of mammals: the complete series," 2002–2003, episode 5: meat eaters.

[11] J. Wertz, *Spacecraft attitude determination and control*. Kluwer Academic Pub, 1978, vol. 73.

[12] G. Oates, *Aircraft propulsion systems technology and design*. AIAA, 1989.

[13] E. Chang-Siu, T. Libby, M. Tomizuka, and R. Full, "A lizard-inspired active tail enables rapid maneuvers and dynamic stabilization in a terrestrial robot," in *Intelligent Robots and Systems (IROS), 2011 IEEE/RSJ International Conference on*. IEEE, 2011, pp. 1887–1894.

[14] T. Mather and M. Yim, "Modular configuration design for a controlled fall," in *Intelligent Robots and Systems, 2009. IROS 2009. IEEE/RSJ International Conference on*. IEEE, 2009, pp. 5905–5910.

[15] T. MathWorks. (2011b) Symbolic math toolbox user's guide. [Online]. Available: http://www.mathworks.com/help/releases/R2011b/pdf_doc/symbolic/symbolic_tb.pdf

[16] E. W. Weisstein. (2012) Lambert w-function. From MathWorld–A Wolfram Web Resource. [Online]. Available: http://mathworld.wolfram.com/LambertW-Function.html

[17] C. Rui, I. Kolmanovsky, and N. McClamroch, "Nonlinear attitude and shape control of spacecraft with articulated appendages and reaction wheels," *Automatic Control, IEEE Transactions on*, vol. 45, no. 8, pp. 1455–1469, 2000.

[18] M. Karami and F. Sassani, "Nonlinear attitude control of an underactuated spacecraft subject to disturbance torques," in *American Control Conference, 2007. ACC'07*. IEEE, 2007, pp. 3150–3155.

[19] A. Jusufi, Y. Zeng, R. Dudley, *et al.*, "Aerial righting reflexes in flightless animals," *Integrative and Comparative Biology*, 2011.

[20] A. Arabyan and D. Tsai, "A distributed control model for the air-righting reflex of a cat," *Biological cybernetics*, vol. 79, no. 5, pp. 393–401, 1998.

[21] C. Chen and N. Sreenath, "Control of coupled spatial two-body systems with nonholonomic constraints," in *Decision and Control, 1993., Proceedings of the 32nd IEEE Conference on*. IEEE, 1993, pp. 949–954.

[22] L. Shampine and M. Reichelt, "The matlab ode suite," *SIAM journal on scientific computing*, vol. 18, no. 1, pp. 1–22, 1997.

[23] M. Srinivasan, "Trajectory optimization, a brief introduction," Powerpoint Presentation at Dynamic Walking Conference, 2010.

[24] A. Valenzuela and S. Kim, "Modular configuration design for a controlled fall," in *Robotics and Automation (ICRA), 2012 IEEE International Conference on*. IEEE, 2012.

[25] C. Walker, C. Vierck Jr, and L. Ritz, "Balance in the cat: role of the tail and effects of sacrocaudal transection," *Behavioural brain research*, vol. 91, no. 1-2, pp. 41–47, 1998.